



UNIVERSIDADE ESTADUAL DE CAMPINAS
SISTEMA DE BIBLIOTECAS DA UNICAMP
REPOSITÓRIO DA PRODUÇÃO CIENTÍFICA E INTELLECTUAL DA UNICAMP

Versão do arquivo anexado / Version of attached file:

Versão do Editor / Published Version

Mais informações no site da editora / Further information on publisher's website:

http://www.scielo.br/scielo.php?script=sci_arttext&pid=S1516-14392018000300023&lng=en&tlng=en

DOI: 10.1590/1980-5373-MR-2017-0848

Direitos autorais / Publisher's copyright statement:

©2018 by Universidade Federal de São Carlos. Departamento de Engenharia de Materiais. All rights reserved.

DIRETORIA DE TRATAMENTO DA INFORMAÇÃO


Cidade Universitária Zeferino Vaz Barão Geraldo

CEP 13083-970 – Campinas SP

Fone: (19) 3521-6493

<http://www.repositorio.unicamp.br>

On the Effect of Aluminum on the Microstructure and Mechanical Properties of CrN Coatings deposited by HiPIMS

Monica Costa Rodrigues Guimarães^a, Bruno César Noronha Marques de Castilho^{a*}, Carlos Cunha^a, Wagner Rafael Correr^b, Paulo Mordente^c, Fernando Alvarez^d, Haroldo Cavalcanti Pinto^a

^aEscola de Engenharia de São Carlos, Universidade de São Paulo, São Carlos, SP, Brasil

^bInstituto de Física de São Carlos, Universidade de São Paulo, São Carlos, SP, Brasil

^cMAHLE Metal Leve, Jundiá, SP, Brasil

^dDepartamento de Física, Universidade Estadual de Campinas, Campinas, SP, Brasil

Received: September 22, 2017; Revised: January 05, 2018; Accepted: February 22, 2018

Hard coatings are a suitable solution for increasing the lifetime of tools and components employed in different industrial applications. Coatings of transition metal nitrides have great use for tribological applications due to their unique mechanical properties. Although widely employed, current deposition methods such as cathodic arc evaporation produce coatings with many defects, which in turn reduce the resistance to wear, especially under severe conditions. High Power Impulse Magnetron Sputtering is a novel physical vapor deposition technique that produces homogeneous coatings. In this study, CrN and CrAlN monolayer coatings were deposited on AISI 304 stainless steel substrates using HiPIMS. X-Ray Diffraction, Scanning Electron Microscopy, Atomic Force Microscopy were used to evaluate the microstructure, phase composition, morphology and chemical composition of the coating. Results showed that HiPIMS is a promising technique to deposit CrN and CrAlN homogeneous coatings with high hardness and good adhesion to the substrate.

Keywords: *HiPIMS, hard coatings, CrN, CrAlN, characterization.*

1. Introduction

Physical Vapor Deposition is a widely used method for coating deposition in industrial scale¹. It consists in the creation of a vapor phase from a target by either evaporation or sputtering. The vapor phase then condensates on a substrate to form the coating or film. The use of magnetrons on the target and the application of high power impulses allows a higher degree of ionization combined with better densification and reduction or full elimination of defects on the coating in a technique called High Power Impulse Magnetron Sputtering (HiPIMS)²⁻⁴.

One of the main strengths of HiPIMS is the use of impulses instead of the continuous power supply, which allows for a higher peak power without melting or causing damages to the target⁵. Another attractive advantage is the possibility to use the ion etching as a previous step before coating deposition. The ion etching promotes a final cleaning of the coating by using high voltage to ionize either argon or metal ions towards the substrate. The collision of these ionized atoms cleans the surface of the impurities that could not be previously removed. This allows a better adhesion of the coating, which cannot be achieved by other Magnetron Sputtering techniques^{2,5,6}.

Amongst the numerous materials that can be sputtered, transition metal nitrides are the most used for tribological applications. Titanium and titanium aluminum nitrides have

been used for high wear resistance applications but failed in high temperature applications with oxidation occurring at 600°C⁷. Therefore, researches have been conducted to explore solutions with higher thermal and chemical stability. Chromium nitride shows promising results for these severe conditions and the addition of aluminum, up to 68%at, acts as a substitutional component in CrN lattice structure and showed improved results with different deposition techniques⁸⁻¹⁰.

The aim of the present work is to characterize monolayer coatings of CrN and CrAlN deposited on stainless steel by HiPIMS and to compare their structural and mechanical properties. X-Ray Diffraction, Scanning Electron Microscopy (SEM), Atomic Force Microscopy (AFM), Nanoindentation and Scratch tests were applied to characterize the coating.

2. Experimental Details

2.1. Materials

HiPIMS deposited CrN and CrAlN coatings on AISI 304 austenitic stainless steel substrates. The 30 mm diameter substrates were ground and polished to a mirror finish (15, 9, 3 and 1 μm diamond paste followed by 0.05 μm silica) and they were ultrasonically cleansed in acetone. The ion etching and depositions were performed in a high vacuum chamber (Plasma-HiPIMS-250) system equipped with 200 mm X

*e-mail: brcn1000@gmail.com.

100 mm pure chromium (99.5%) and chromium aluminum (99.5%) targets with 50-50at% composition. Substrates were placed at the substrate holder at a distance of 65mm from the target. A base layer of Cr was used for the CrN coating and a CrAl for the CrAlN coating to provide better adhesion.

2.2. Coating process

The chamber was heated up to 400°C at a pressure of 1.0Torr for the ion etching process. Base layer and coating deposition parameters are described in Tab. (1). The working pressure was 4mtorr throughout the deposition process. The flow rate of argon and nitrogen was 40 and 50 sccm, respectively. The HiPIMS frequency was set to 400 Hz.

2.3. Characterization

The film crystalline structure was investigated by X-Ray Diffraction (XRD) using a MRD-XL Diffractometer (PANalytical, the Netherlands), with a Bragg-Brentano configuration (θ -2 θ) and parallel beam geometry. The X-Ray parallel beam of 3x3mm² was produced by a Co-K α radiation (1.78897Å, 40kV and 40mA) with a 2 θ range from 34° to 110°, step size 0.05° and at 10s per step. XRD analysis was used for evaluation of preferred orientation growth. The calculations to determine texture coefficient utilized the equations proposed by Birkholz¹¹ by means of the equations (1) and (2).

$$T_{(hkl)} = \frac{I_{hkl}^m / A_{\theta 2\theta}(\theta_{hkl})}{I_{hkl}^{ICDD}} \frac{\sum_{hkl} I_{hkl}^{ICDD}}{\sum_{hkl} I_{hkl}^m / A_{\theta 2\theta}(\theta_{hkl})} \quad (1)$$

$$A_{\theta 2\theta}(\theta_{hkl}) = \left(1 - \exp\left(\frac{-2\mu t}{\sin\theta}\right)\right) \quad (2)$$

In those equations, μ is the linear absorption coefficient ($\mu_{Cu} = 1215\text{cm}^{-1}$), t is the film thickness, and I is the intensity of hkl plane either on the powder pattern (index ICDD) or the measured one (index m).

A Field-Emission Scanning Electron Microscope (FEG-SEM) Inspect F-50 (FEI, The Netherlands) was used to characterize the morphology at the top and the cross-section of the coatings.

The coating composition was measured by X-Ray Energy Dispersive spectrometer (Apollo X SDD, EDAX, USA) using a standard sample of CrN to calibrate the measurement. Surface roughness was calculated from AFM images obtained in a Nanosurf FlexAFM (Nanosurf, Switzerland). A PB 1000 nanoindenter (Nanovea, USA) equipped with a Berkovich diamond indenter was used to measure hardness. For each

sample, twenty points separated by a distance of 15 μm were measured with a load of 150mN at the top and 50mN at the cross-section and the average hardness and standard deviation were calculated. To evaluate the adhesion of the coatings to the substrate, scratch tests were carried out using the same NanoveaPB 1000. The tests were performed with conical diamond indenter (200 μm radius) using progressive load from 0N to 100N at a loading rate of 100N/min and the scratch length of 4mm.

3. Results and Discussion

3.1. EDX analysis

Table (2) presents the chemical composition of the coatings measured by EDX analysis. The values are close to the expected stoichiometry. For CrN coating a 50-50at% composition was expected and for the CrAlN coating the composition was expected to be 50at% of nitrogen and 25at% of chromium and aluminum. The N₂ and Ar flow rate are the main responsible for the deposited content of nitrogen and the metals, respectively¹²⁻¹⁴. Therefore, the measured values indicate a correct adjustment between the flow rate of nitrogen and the sputtering rate of the metals adjusted by the flow rate of argon.

Table 2. Results of EDX analysis showing stoichiometric composition.

Chemical composition [at%]	Chemical composition [at%]		
	Cr	Al	N
CrN	49.36	-	50.64
CrAlN	26.83	26.38	46.79

3.2. XRD analysis

Figure (1) illustrates the XRD patterns of the coating CrN (a) and CrAlN (b). By comparing the result of the diffractogram with the powder pattern, a decrease in the 2 θ values and a correspondent increase in the d-spacing was found. This can be attributed to a Poisson effect caused by the strain on the plane perpendicular to the direction of measurement. On the other hand, CrAlN coating show the opposite behavior, with a decrease in the interplanar spacing. Two opposite phenomena are acting in the lattice structure of the CrAlN coating. The coating is probably under compressive stress, which is a characteristic of magnetron sputtering coatings, which in turn contribute to the same effect observed for the CrN. However, the presence of Al acting as substitutional

Table 1. Process parameters for sample deposition.

Sample	Ion Etching			Base Layer Deposition				Coating Deposition				
	Time (h)	Bias (V)	Atmosphere	Time (h)	Bias (V)	Atmosphere	T (°C)	Time (h)	Bias (V)	Atmosphere	T (°C)	Hipims (W)
CrN	02:00	450	Ar	01:30	80	Ar	400	13:30	-80	Ar / N ₂	400	970
CrAlN	02:00	450	Ar	01:30	80	Ar	400	13:30	-80	Ar / N ₂	400	1020

element on the lattice structure reduces the lattice parameter causing a shift in the 2θ values⁸. It is evident that the latter is more pronounced and therefore the shift to higher values of 2θ is observed.

The texture coefficient was calculated based on the diffractograms in Figure 1. The results are shown in Figure 2. The change of preferred orientation growth can be observed by both Figures. Whilst CrN shows texture on the (311) plane, CrAlN texture coefficient is close to 1 to almost all planes, which means it is close to the powder diffraction pattern. Furthermore, for CrAlN, (222) plane has predominant growth.

3.3. Microstructure

Figure (3) shows SEM images of CrN (a and c) and CrAlN (b and d) from cross-section and top view. The microstructure of CrAlN coating on substrate surface from top view shows smaller grains than CrN. No growth defects (droplet) can be observed on the film surface and both shows a dense microstructure although they presented some inter-columnar voids. Cross-section images (Fig.3 (a), (b)) show columnar structure.

The coatings thickness were measured according to the Fig. 3 (a) and (b). CrN coating presented a thickness of $16.6 \pm 0.2 \mu\text{m}$ while CrAlN had $18.8 \pm 0.2 \mu\text{m}$ thickness. This means that, as the deposition time is the same for both samples, CrAlN showed higher deposition rate, which in principle contradicts the literature. The slightly higher applied power could be the reason for such discrepancy.

Surface morphology of the coatings was studied using AFM. In Fig. (4) (a) and (b) are shown the 3D AFM images of CrN and CrAlN respectively. The root mean square (RMS) roughness values are $0.239 \mu\text{m}$ and $0.158 \mu\text{m}$ whilst the average roughness (R_a) shows $0.184 \mu\text{m}$ and $0.120 \mu\text{m}$ for CrN and CrAlN respectively. The value for the CrAlN coating is smaller than for the CrN coating and it is related

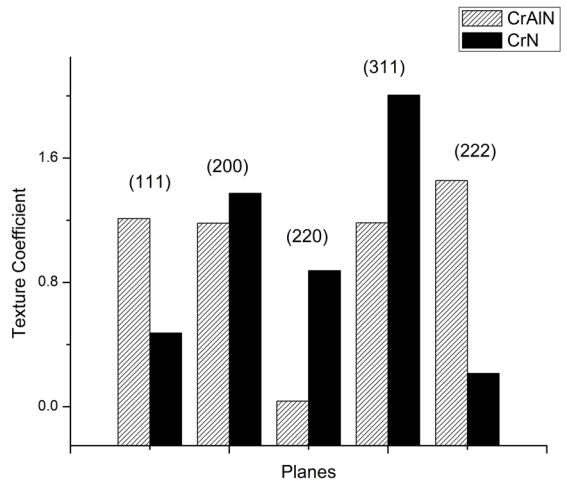


Figure 2. Texture coefficient showing preferential orientation growth on (311) plane for CrN coating

to the fact that the CrAlN coating has smaller columnar grains when compared to the CrN.

3.4. Mechanical and tribological properties.

3.4.1. Nanohardness

The nanohardness tests were carried out for the CrN and CrAlN monolayer coatings on the cross-section and at the top surface using a Berkovich diamond indenter. CrN and CrAlN coatings displayed on the cross-section hardness values of $(12 \pm 2) \text{GPa}$ and $(13 \pm 3) \text{GPa}$, respectively. At the top surface the measured hardness values were $(12 \pm 1) \text{GPa}$ for CrN and $(16.5 \pm 2) \text{GPa}$ for CrAlN. The difference between the hardness values from the top and the cross-section for CrAlN indicates the anisotropy of the coating, which is expected due to the characteristic columnar and epitaxial

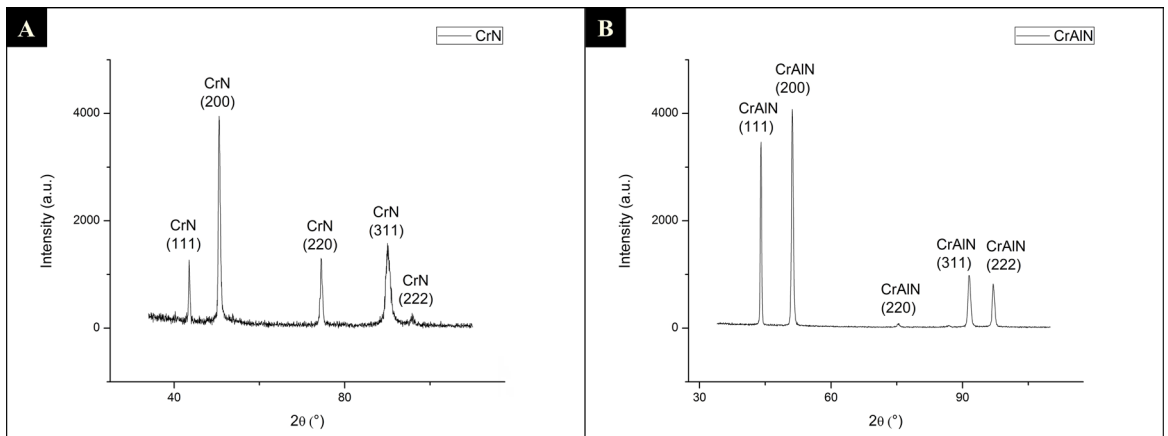


Figure 1. XRD analysis of (A) CrN and (B) CrAlN coatings

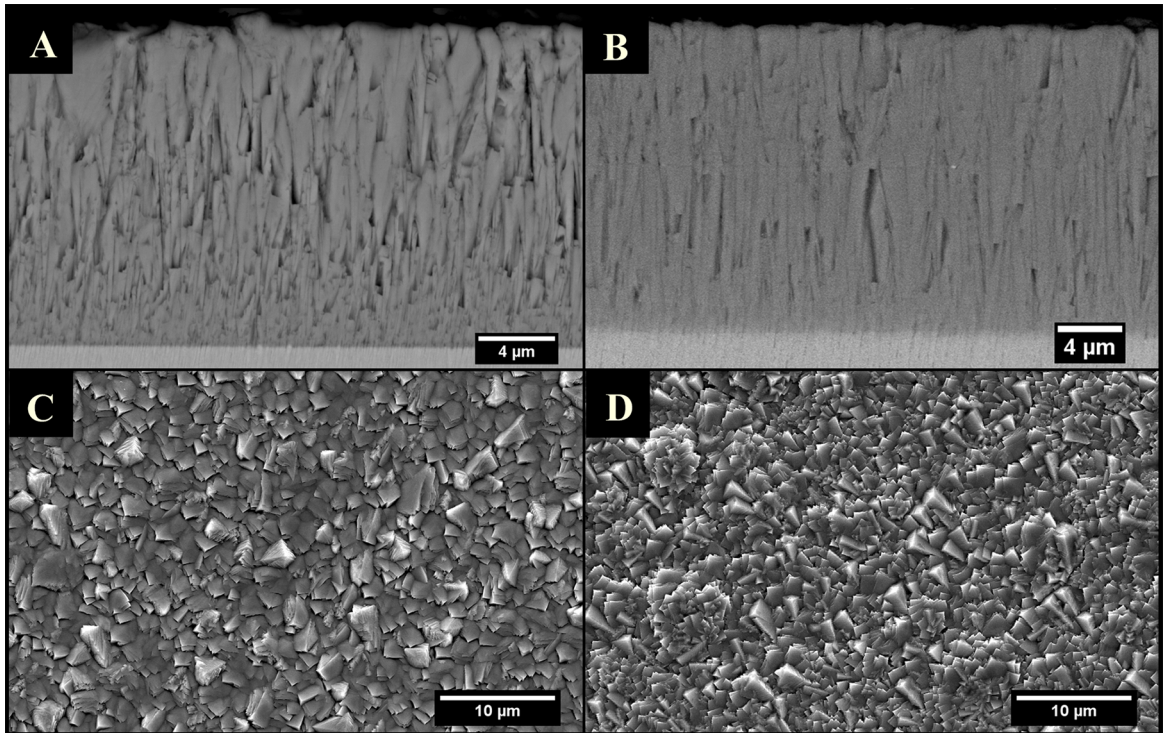


Figure 3. SEM images of cross-section of (A) CrN and (B) CrAlN, and the surface morphology of (C) CrN and (D) CrAlN

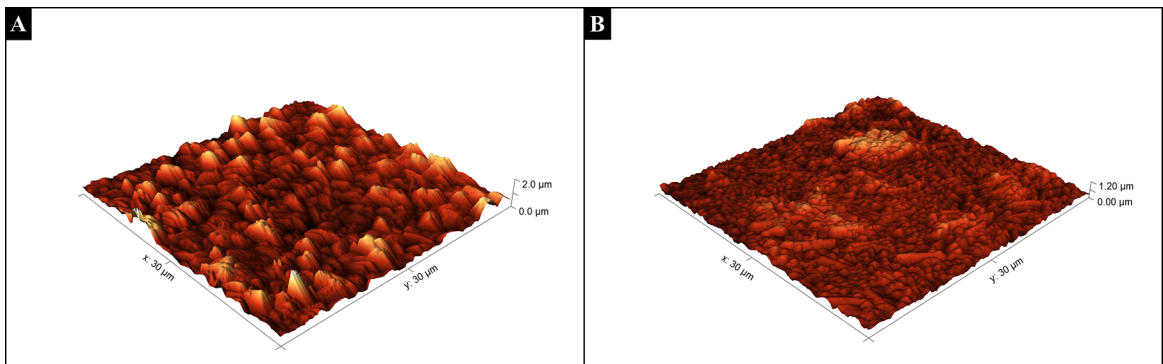


Figure 4. AFM Images of the surface of (A) CrN and (B) CrAlN films. CrN shows higher mean roughness

growth of magnetron sputtered coatings. Better conditions of the energy and the flux of ion bombardment for CrN coatings, such as an increase of the bias voltage, can ensure higher hardness and better mechanical properties because of high coating density, without voids in the microstructure. The increase of the bias also promotes a change in preferred orientation from (100) to (220) showing high hardness and high residual compressive stress^{15,16}.

The difference of hardness between CrN and CrAlN can be attributed to the presence of aluminum on the latter. The addition of aluminum up to 68% increases the hardness of the coating by solid solution, due to the lattice deformation. After that, the aluminum forms an AlN hexagonal phase, which reduces the coating hardness^{17,18}. As the percentage of aluminum was below this value, a higher hardness was found on the CrAlN coating.

3.4.2. Scratch

Three scratch tests were performed 2mm apart for both CrN and CrAlN coatings. Critical load (L_c) measurements for adhesion strength were 34.5N and 46N respectively. Both coatings failed by delamination as can be observed from Fig.(5), which indicates adhesion failure. The higher value achieved by CrAlN coating indicates better adhesion to the substrate than the CrN coating. The lack of cohesive failure in both cases indicates the high homogeneity of the coatings. The lower values of L_c obtained in this work, in comparison with other similar studies, can be attributed to the pores in the coating and the voids are not advantageous for good adhesion. In addition, the bias may not have been sufficient to etch away the oxides of the substrate. Despite that, the coatings showed better results than those deposited by other techniques^{2,5,13}.

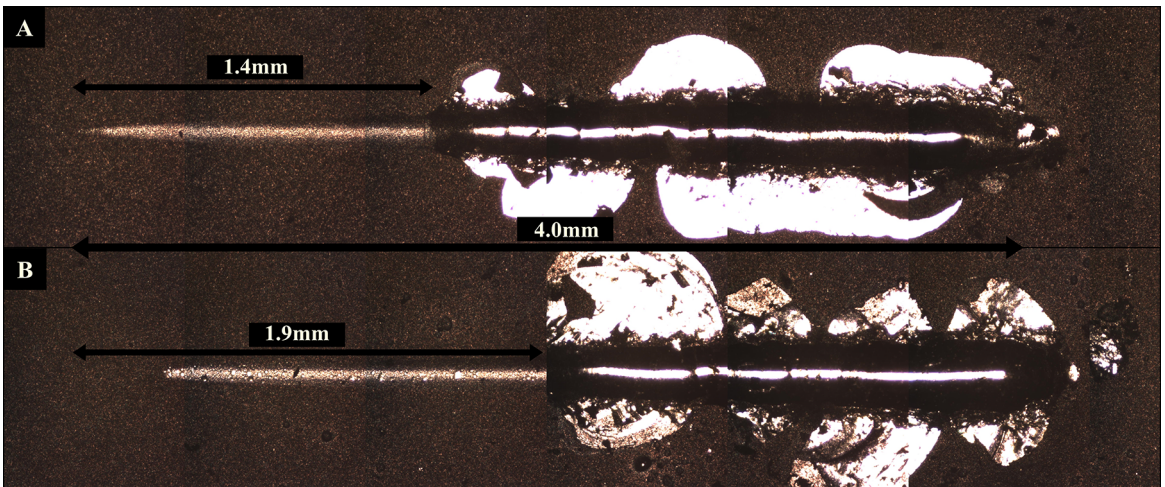


Figure 5. Scratch test on (A) CrN and (B) CrAlN coatings. CrAlN showing better adhesion than CrN coating

4. Conclusions

In this study, CrN and CrAlN monolayer coatings were produced using the HiPIMS technique. The CrAlN coating showed higher hardness, lower surface roughness and better adhesion to the substrate than the CrN coating. The XRD data showing peak shifts on the 2θ scale and the lack of AlN peaks in the CrAlN coating confirms the presence of aluminum as a substitutional element in the CrN lattice structure. CrAlN deposited by HiPIMS shows promising results towards its applications as a high wear resistance coating. Further studies will correlate the hardness and adhesion of the coating with the residual stresses and texture and the optimization of these properties as a function of various deposition parameters.

5. Acknowledgements

The Authors would like to thank MAHLE Metal Leve and BNDES (Decision Dir. 640/2012) for funding. MCRG and BCNMC acknowledge CAPES and CNPq for the scholarships. HP is a CNPq fellow.

6. References

- Rodríguez RJ, García JA, Medrano A, Rico M, Sánchez R, Martínez R, et al. Tribological behaviour of hard coatings deposited by arc-evaporation PVD. *Vacuum*. 2002;67(3-4):559-566.
- Helmersson U, Lattermann M, Bohlmark J, Ehisarian AP, Gudmundsson JT. Ionized physical vapor deposition (IPVD): A review of technology and applications. *Thin Solid Films*. 2006;513(1-2):1-24.
- Mishra B, Moore JJ, Lin JL, Sproul WD. Advances in Thin Film Technology through the Application of Modulated Pulse Power Sputtering. *Materials Science Forum*. 2010;638-642:208-213.
- Ehisarian AP, Münz WD, Hultman L, Helmersson U, Petrov I. High power pulsed magnetron sputtered CrN_x films. *Surface and Coatings Technology*. 2003;163-164:267-272.
- Sarakinos K, Alami J, Konstantinidis S. High power pulsed magnetron sputtering: A review on scientific and engineering state of the art. *Surface and Coatings Technology*. 2010;204(11):1661-1684.
- Ehisarian AP, Wen JG, Petrov I. Interface microstructure engineering by high power impulse magnetron sputtering for the enhancement of adhesion. *Journal of Applied Physics*. 2007;101(5):054301.
- Xu YX, Riedl H, Holec D, Chen L, Du Y, Mayrhofer PH. Thermal stability and oxidation resistance of sputtered Ti-Al-Cr-N hard coatings. *Surface and Coatings Technology*. 2017;324:48-56.
- Kimura A, Kawate M, Hasegawa H, Suzuki T. Anisotropic lattice expansion and shrinkage of hexagonal TiAlN and CrAlN films. *Surface and Coatings Technology*. 2003;169-170:367-370.
- Ehisarian AP, Hovsepian PE, Hultman L, Helmersson U. Comparison of microstructure and mechanical properties of chromium nitride-based coatings deposited by high power impulse magnetron sputtering and by the combined steered cathodic arc/unbalanced magnetron technique. *Thin Solid Films*. 2004;457(2):270-277.
- JakubčzyováD, HagarovaM, Hvizdoš P, CervováJ, FrenákM. Tribological Tests of Modern Coatings. *International Journal of Electrochemical Science*. 2015;10(9):7803-7810.
- Birkholz M. *Thin Film Analysis by X-Ray Scattering*. Weinheim: Wiley-VCH; 2006.
- Pulugurtha SR, Bhat DG. A study of AC reactive magnetron sputtering technique for the deposition of compositionally graded coating in the Cr-Al-N system. *Surface and Coatings Technology*. 2006;201(7):4411-4418.
- Zhang ZG, Rapaud O, Bonasso N, Mercs D, Dong C, Coddet C. Control of microstructure and properties of dc magnetron sputtering deposited chromium nitride films. *Vacuum*. 2008;82(5):501-509.
- Shah HN, Jayaganthan R, Kaur D, Chandra R. Influence of sputtering parameters and nitrogen on the microstructure of chromium nitride thin films deposited on steel substrate by

- direct-current reactive magnetron sputtering. *Thin Solid Films*. 2010;518(20):5762-5768.
15. Grasser S, Daniel R, Mitterer C. Microstructure modifications of CrN coatings by pulsed bias sputtering. *Surface and Coatings Technology*. 2012;206(22):4666-4671.
 16. Kong Q, Ji L, Li H, Liu X, Wang Y, Chen J, et al. Influence of substrate bias voltage on the microstructure and residual stress of CrN films deposited by medium frequency magnetron sputtering. *Materials Science and Engineering: B*. 2011;176(11):850-854.
 17. Ding XZ, Zeng XT. Structural, mechanical and tribological properties of CrAlN coatings deposited by reactive unbalanced magnetron sputtering. *Surface and Coatings Technology*. 2005;200(5-6):1372-1376.
 18. Cavaleiro A, de Hosson JT, eds. *Nanostructured Coatings*. New York: Springer; 2006.